

## Electronic Supporting Material on the Biosensors and Bioelectronics

### publication entitled

### Real time monitoring of glucose in whole blood by smartphone

*Miguel M. Erenas<sup>\*1,2</sup>, Belén Carrillo Aguilera<sup>1</sup>, Kevin Cantrell<sup>3</sup>, Sara Gonzalez-Chocano<sup>1</sup>, Isabel Perez de Vargas Sansalvador<sup>1,2</sup>, Ignacio de Orbe-Payá<sup>1,2</sup> and Luis Fermin Capitan-Vallvey<sup>1,2</sup>.*

<sup>1</sup> ECsens. Department of Analytical Chemistry.<sup>2</sup> Unit of Excellence in Chemistry applied to Biomedicine and the Environment of the University of Granada. Campus Fuentenueva, Faculty of Sciences, 18071, University of Granada, Spain.

<sup>3</sup> Department of Chemistry. The University of Portland, 5000 N Willamette Blvd, Portland, OR 97203, USA.

\*Corresponding author, email: [erenas@ugr.es](mailto:erenas@ugr.es)Table of Contents

1.	App description .....	2
2.	White balance .....	4
3.	Devices optimization .....	5
3.1.	Detection and transduction mechanism.....	5
3.2.	TMB retention .....	6
3.3.	TMB and HRP optimization.....	7
3.4.	pH adjustment.....	7
3.5.	GOx optimization .....	8
3.6.	Volume of sample.....	8
3.7.	Calibration .....	9
3.8.	Stability.....	10
3.9.	Plasma separation .....	10
3.10.	Whole blood calibration .....	11
3.11.	Interfering species .....	11
4.	Real samples.....	13
5.	Sensor cost.....	13
6.	References .....	15

## 1. App description

Two versions of image processing software were written for use with this sensor. The PC based version was written using the Anaconda distribution of Python 2.7 (<https://www.anaconda.com/>) in conjunction with the Python/Windows interface to the Open Source Computer Vision Library version 3.2.0 (<https://opencv.org/>). The Android based version was written using Android Studio (<https://developer.android.com/studio/index.html>) in conjunction with Android/Java wrapper for the OpenCV library. In the discussion that follows all functions mentioned are OpenCV functions unless otherwise noted. The primary difference between the versions is that the Android app is designed to run natively on a variety of smartphones in real-time where the PC version is designed to work with recorded videos from any recorded source (including a smartphone) and to provide diagnostic data useful in the development of the devices. Thus, in the interest of processing speed and time resolution, some of the image processing steps are omitted from the final Android version.

The OpenCV library function `cvtColor` was used to convert from the RGB color space to the HSV color space. Note that in the Python/Windows interface to OpenCV that the Hue values of the HSV color space have a range of 0 to 179, but in the Java version (as with all other tristimulus values) the range is 0 to 255. The region of interest (ROI) was automatically identified based on their Saturation value in the HSV color space that is defined as RGB values (max-min) divided by the largest RGB value (max). Pixels with Saturation greater than ~16% of the possible range were flagged as colored and included in the region of interest. (Note that the threshold saturation is smaller and adjustable in the PC program, and lower values will result in earlier detection of the color forming reaction. This early detection of pixels that are only slightly colored is only possible when the white balance of the image is correct – see later discussion.) Red pixels, those with a Hue within ~12% of the red origin, were excluded from the region of interest. Thus, in the Android app with a hue scale of 0 to 255, only pixels with a Hue between 31 and 224 and Saturation greater than 39 were included in the region of interest. The OpenCV library function `inRange` was used to calculate a Boolean mask of the image subject to these constraints. Groups of contiguous pixels in the resulting mask were found using the `findContours` function, and the largest area group (the one with the most pixels as calculated with the `contourArea` function) was identified as the sensor region of interest. For display in the app, the largest contour is outlined in red, and a green bounding rectangle is drawn around it. The unchanged (but rescaled by a factor of 2) frame image is displayed in the upper left quarter of the screen. This frame image with non-ROI pixels masked as black is displayed in the lower left quarter of the screen. Only pixels inside the region of interest were used in subsequent data manipulations (Figure S1).



**Figure S1.**  $\mu$ TPAD after the dropping of a whole blood sample and the ROI detected by the app.

For a particular frame, the histograms of RGB, HSV, and absorbance ratios for pixels in the region of interest were calculated using the `calcHist` function and displayed using the functions `normalize` and `line` by drawing directly onto the displayed image. Absorbance ratio is defined as the negative common logarithm of the ratio of pairings of two color coordinates. To avoid undefined values, all zero value tristimulus values were first changed to a value of one. Then the three color absorbance values, here defined as  $cA1=cA(b/g)$ ,  $cA2=cA(g/r)$ , and  $cA3=cA(b/r)$  were calculated and are hereafter referred to as  $cA123$ .

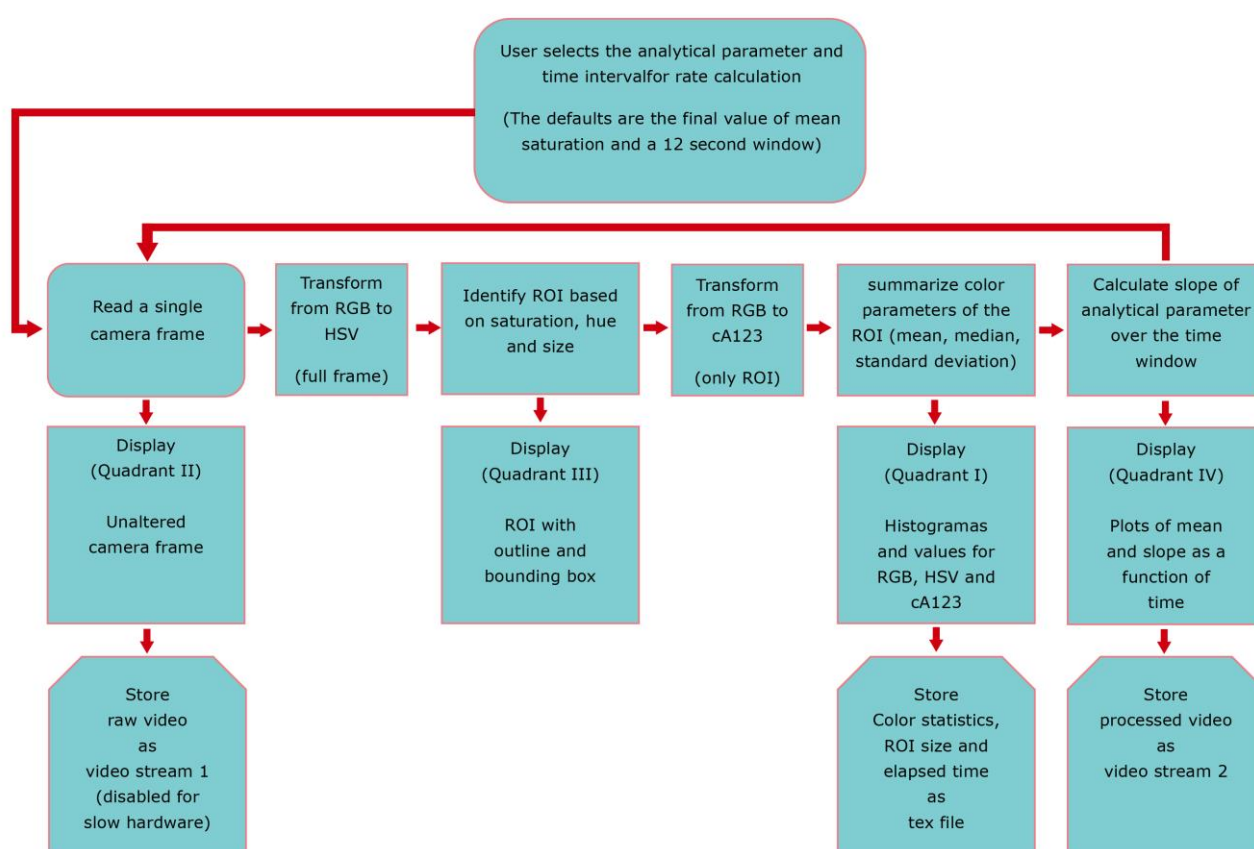
For the Android app, designed to run on a variety of hardware and display data in real-time, the elapsed time of a particular video frame is defined as the current system time (as reported by the Android System function `nanoTime`) minus the system time when the camera view started. For recorded videos with fixed frame rate compression, this function is only called once, and a running count of the frame number is used along with the frame rate to calculate the elapsed time.

While the video is being analyzed, the mean and standard deviation of all color values (RGB, HSV, and  $cA123$ ) of pixels inside the region of interest for a single video frame are displayed on the screen and recorded in a text file along with the elapsed time for that frame (hereafter referred to as frame means). For the glucose sensor, two analytical parameters were considered: saturation from the HSV color space and color absorbance for the blue/red ratio ( $cAb/r$  or  $cA3$ ). Saturation is likely to be more robust in terms of lighting conditions, and it was selected as the default analytical parameter. A running plot of RGB values and the analytical parameter are plotted as a function of elapsed time.

For the rate calculation a subset of the data from 12 s before the elapsed time up to and including the current frame is defined. The mean of the frame means within this twelve second window is then calculated. In the Android app, this is a simple moving average that lags behind the current frame mean by approximately 5 s. A least-squares linear fit to the analytical parameter versus time within the 12s window was also calculated using the `solve` function configured to use singular value decomposition for matrix inversion. The slope of the best fit line was taken to be the rate of change in the sensor response. Both the moving average of the analytical parameter and the rate of change

are displayed as separate auto-scaling plots in the lower right of the display. In the moving average plot, if the absolute value of the slope is less than a threshold value (e.g. less than 0.001 for cA(b/r)), the value is considered stable and plotted in green. If the slope is larger than the threshold, the moving average is plotted in red (increasing). The moving average is plotted in blue when the slope is less than the negative threshold (decreasing).

Additionally, the processed video is stored as a separate video file. In the Android app the raw video file can be stored additionally (recording both the raw and processed video does reduce the frame rate for both files). The summary data for each frame, the rolling average, and the slope are also stored as a comma separated text file.



**Scheme 1.** App flow diagram.

## 2. White balance

To optimize the white balance setting selected on the digital camera, we compared the signal variation between two different H<sub>2</sub>O<sub>2</sub> concentrations, 10 and 500 μM. Each thread was treated with 0.35 μL of 0.05 U/mL HRP and 0.35 μL of 20.8 mM TMB. Once the devices were dry, 10 μL of either 10 or 500 μM H<sub>2</sub>O<sub>2</sub> were added. The saturation was obtained from each H<sub>2</sub>O<sub>2</sub> solution using 4 different white

balance settings: incandescent (2800K), sun light (5500K), cloudy light (6500K) and fluorescent light (4000K) and the difference in signal was calculated. As expected due to the color temperature of the illumination used in the study, the larger signal difference was observed when incandescent white balance was used (Figure S2).

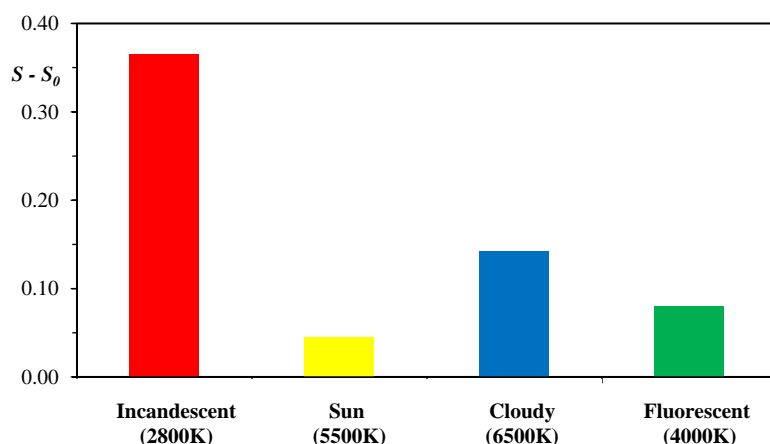
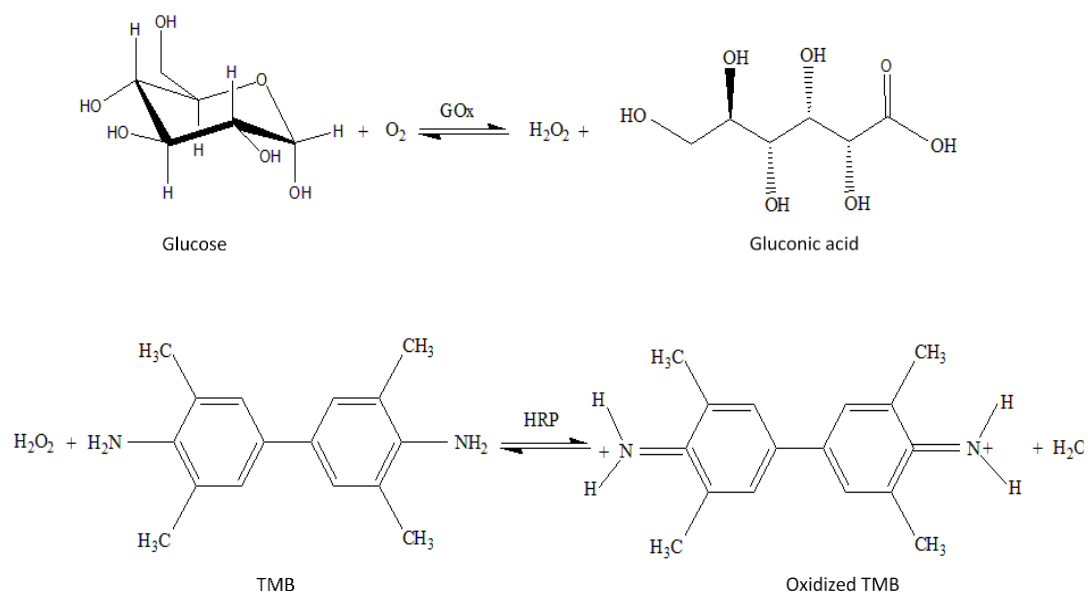


**Figure S2.** White balance study using TMB optimization conditions.  $S_0$ : saturation of the thread just prepared;  $S$ : saturation of the thread after reaction with  $H_2O_2$ .

### 3. Devices optimization

#### 3.1. Detection and transduction mechanism

The method implemented in the  $\mu$ TPAD is glucose oxidase (Burtis, A et al., 2008), based on two different reactions, detection and transduction. In the detection reaction, the GOx enzyme reacts with the glucose in the sample, obtaining gluconic acid and  $H_2O_2$ . Both are colorless, which is why the transduction reaction is needed, where the  $H_2O_2$  generated together with the HRP enzyme reduces the TMB, obtaining a blue compound. The color generated throughout the entire process is proportional to the glucose concentration in the sample.



**Scheme S2.** Recognition and transduction mechanism

### 3.2. TMB retention

To retain TMB on thread the following reagents were added (in order), 0.35  $\mu\text{L}$  of 0.05 U/mL HRP, 0.35  $\mu\text{L}$  of 20.8 mM TMB and, finally, 0.7  $\mu\text{L}$  of chitosan solution. Chitosan concentrations tested were 0, 1, 5, 10 and 15 mg/mL, and three  $\mu\text{TAD}$  were prepared from each one. Once the devices were dry, 10  $\mu\text{L}$  of 50 mM  $\text{H}_2\text{O}_2$  was added. The color change of the thread was recorded using the Sony digital camera, and the length of the colored zone was measured and compared.

**Table S1.** Average length of the ROI depending on the chitosan used to retain TMB on thread and CV (n=3).

Chitosan ( $\mu\text{g}$ )	Length (cm)	CV (%) (n=3)
0	1.4	20.3
0.7	1.2	3.6
3.5	1.3	11.0
7.0	1.4	7.8
10.5	1.3	17.5

### 3.3. TMB and HRP optimization

TMB and HRP were optimized simultaneously using a factorial design. Concentrations tested were: TMB 1.0, 2.1, 5.0, 10.0 and 20.8 mM; and HRP  $1.0 \cdot 10^{-2}$ ,  $2.0 \cdot 10^{-2}$ ,  $3.0 \cdot 10^{-2}$ ,  $4.0 \cdot 10^{-2}$  and  $5.0 \cdot 10^{-2}$  U/mL. The  $\mu$ TADs were prepared by adding 0.35  $\mu$ L of HRP, 0.35  $\mu$ L of TMB mM and 0.7  $\mu$ L of chitosan. All 25 different  $\mu$ TAD prepared with HRP and TMB were tested by adding 10  $\mu$ L of 50 mM  $H_2O_2$  solution with three replicates per  $\mu$ TAD composition. The color change was monitored using the Sony digital camera and analyzed using ImageJ software.

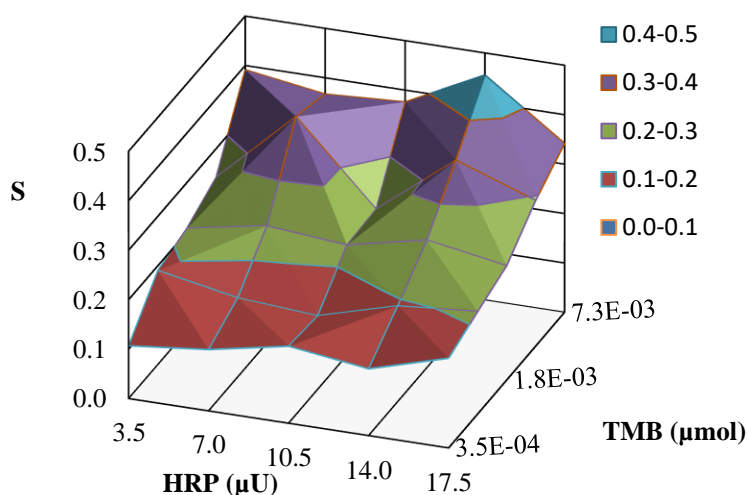


**Figure S3.** Factorial design for TMB and HRP optimization in the  $\mu$ TAD.

### 3.4. pH adjustment

To adjust the pH of the sample in the  $\mu$ TAD, different volumes of 1xPBS buffer were immobilized by drying. After adding  $H_2O_2$  standard solution and measuring the pH at the end of the thread, we concluded that the immobilization of 5  $\mu$ L is enough to buffer the sample. Subsequently, the S value obtained using the immobilized buffer was compared with a buffered  $H_2O_2$  solution at the working pH (7.4). In the first case, 5  $\mu$ L of 1xPBS was added and, after waiting 10 minutes, 0.35  $\mu$ L HRP solution, 0.35  $\mu$ L of TMB of the previously optimized concentrations, and 0.7  $\mu$ L of 1 mg/mL chitosan solution were added. On the second one, only reagents and no buffer were used. The prepared  $\mu$ TAD were tested with 5, 15, 25, 50, 100, 125, 150 and 250  $\mu$ M  $H_2O_2$  solutions, three replicates each, monitoring the color change as previously with a Sony digital camera.

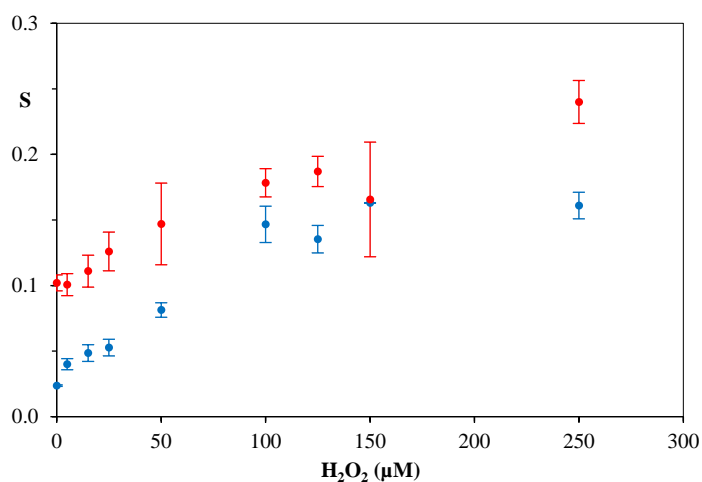


**Figure S4.** Influence of buffer location on the response of the  $\mu$ TAD (n=3). Blue dots: buffer in the device; red dots: buffer in solution.

### 3.5. GOx optimization

The GOx concentrations assayed were 0.026, 0.029, 0.044, 0.087, 0.870, and 1.740 U/ $\mu$ L. Different  $\mu$ TADs were prepared by the adding (in order) 5.0  $\mu$ L of 1xPBS, 1  $\mu$ L of GOx, 0.35  $\mu$ L of 0.04 U/mL HRP, 0.35  $\mu$ L of 20.8 mM TMB, and 0.7  $\mu$ L of 1 mg/mL chitosan solution. For testing the device, three replicates of 10  $\mu$ L of 250  $\mu$ M glucose solution were added, and the color change was recorded over time in a video file using the Sony digital camera.

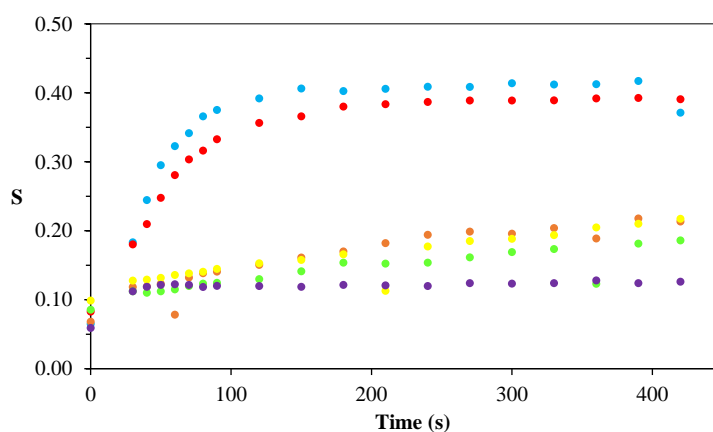


**Figure S5.** Response of the  $\mu$ TAD over time depending on GOx concentration. Blue dots: 1.740 U/ $\mu$ L; red dots: 0.870 U/ $\mu$ L; orange dots: 0.087 U/ $\mu$ L; green dots: 0.044 U/ $\mu$ L; yellow dots: 0.029 U/ $\mu$ L and purple dots: 0.026 U/ $\mu$ L.

### 3.6. Volume of sample

Volumes tested were 5.0, 7.5, 10.0, 12.5, 15.0, 17.5 and 20.0  $\mu$ L of 250  $\mu$ M glucose using  $\mu$ TAD with 5.0  $\mu$ L of 1xPBS, 1  $\mu$ L of 1.740 U/ $\mu$ L GOx, 0.35  $\mu$ L of 20.8 mM TMB and 0.35  $\mu$ L of 0.04 U/mL HRP and 0.7  $\mu$ L of 1 mg/mL chitosan (n=3).

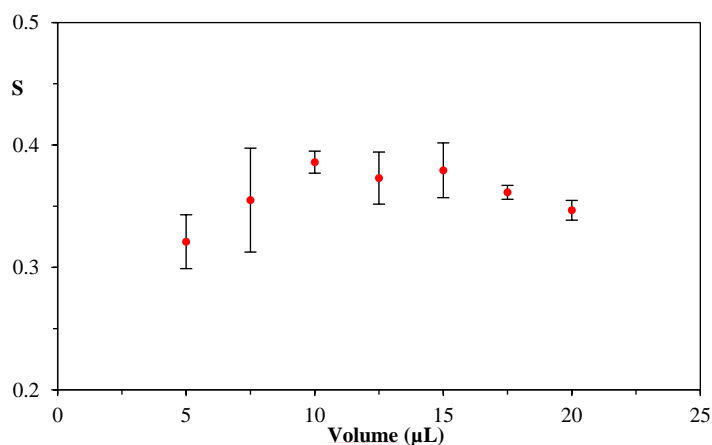


**Figure S6.** Influence of volume of sample.

### 3.7. Calibration

Ten different glucose standards (1, 5, 15, 25, 50, 100, 125, 250, 500 and 1000  $\mu\text{M}$ ) were used to calibrate the  $\mu\text{TAD}$  and prepared as follows: 1.0  $\mu\text{L}$  of 1.74  $\text{U}/\mu\text{L}$  GOx was added to the recognition region followed by 0.35  $\mu\text{L}$  of 20.8 mM TMB in ethanol, 0.35  $\mu\text{L}$  of  $3.5 \cdot 10^{-2}$   $\text{U}/\text{mL}$  HRP and, after waiting one minute, 0.7  $\mu\text{L}$  of 1 mg/mL chitosan aqueous solution were added to the transduction region. Finally, it was dried at room temperature in dark conditions. Then, 10  $\mu\text{L}$  of sample are added to the sampling region and the color of the  $\mu\text{TAD}$  is captured and analyzed using a Smartphone and the custom Android-based app developed. Figure S7 shows the calibration function using S as analytical parameter for equilibrium signal.

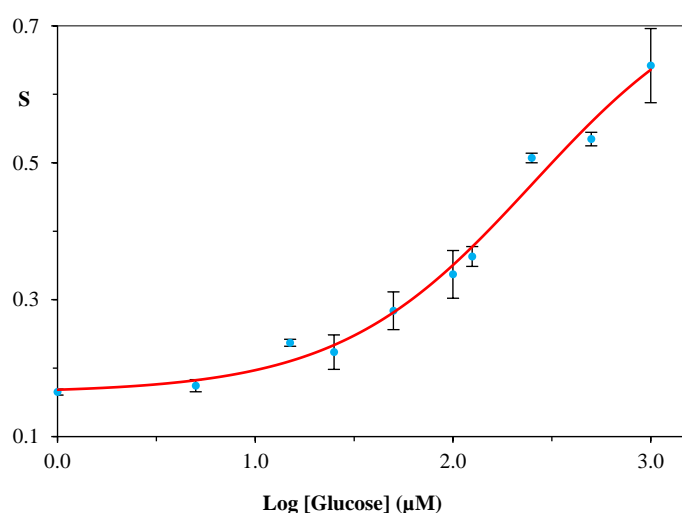


**Figure S7.** Calibration obtained using S as analytical parameter obtained 100 s after the sample addition.

### 3.8. Stability

A stability study was performed in order to characterize the lifetime of the  $\mu$ TAD after its preparation. For this purpose, the stability was studied for 78 days in two different conditions: a) preserving the  $\mu$ TAD in the fridge and b) preserving the  $\mu$ TAD in a desiccator. Results obtained are shown in Figure S8, showing that the device is not stable over time, the signal decays to the 50% the day after the preparation of the  $\mu$ TAD. Due to the low stability of the enzymes, it may be beneficial to protect them in some structure such as enzyme co-embedded organic–inorganic hybrid materials (nanoflowers) (Ariza-Avidad et al., 2016; Zhu et al., 2017).

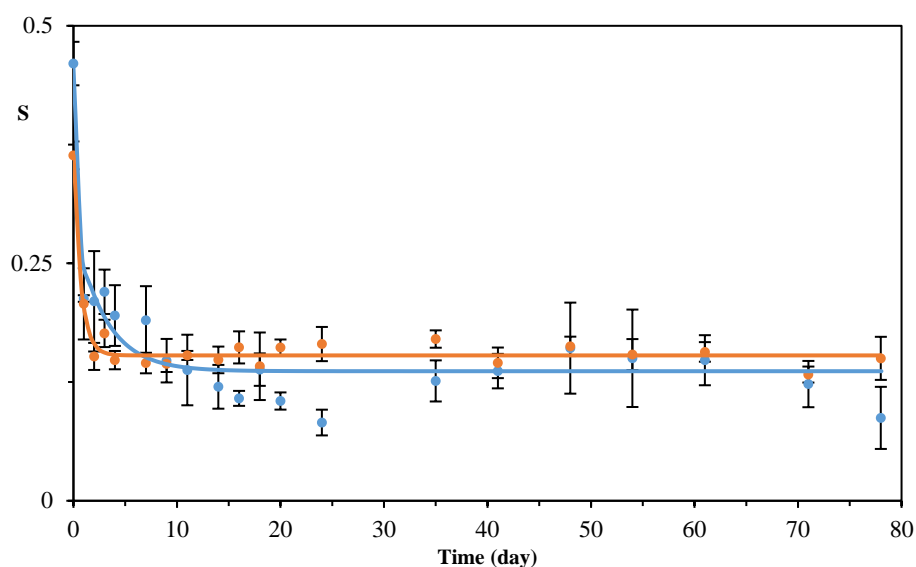


**Figure S8.** Lifetime study of  $\mu$ TAD. Blue line and dots,  $\mu$ TAD preserved in fridge; orange line and dots,  $\mu$ TAD preserved in desiccator.

### 3.9. Plasma separation

Different volumes and concentrations of NaCl and EDTA were immobilized by drying on the thread, and different volumes of blood were assayed in order to perform the plasma separation with no successful results. (Figure S9). In all the assays performed, the RBC flow together with the plasma through the thread, and separation is not achieved.

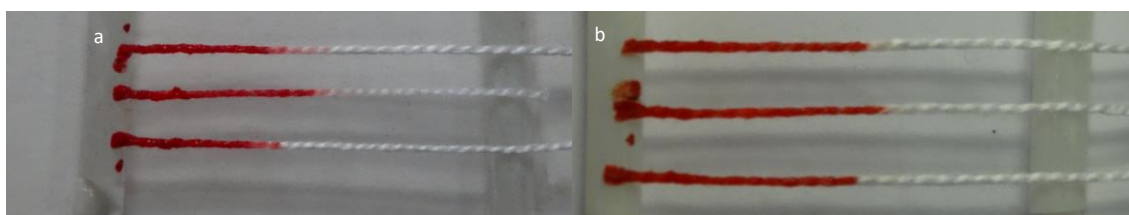


**Figure S9.** Assays performed using NaCl (a) and EDTA (b) to perform the RBC separation from plasma on thread.

For the LF1 membrane, different volumes of blood sample were tested: 7, 6, 5, 4, 3, 2, 1, 0.75 and 0.5  $\mu\text{L}$ . When 7 to 4  $\mu\text{L}$  of blood were used, the RBC exceeded the membrane capacity and broke through to the thread (Figure S10). In case of volumes from 2 to 0.5  $\mu\text{L}$  of whole blood, it was not enough to get serum on thread. Only in case of 3  $\mu\text{L}$ , plasma free of RBC was drawn onto the thread.

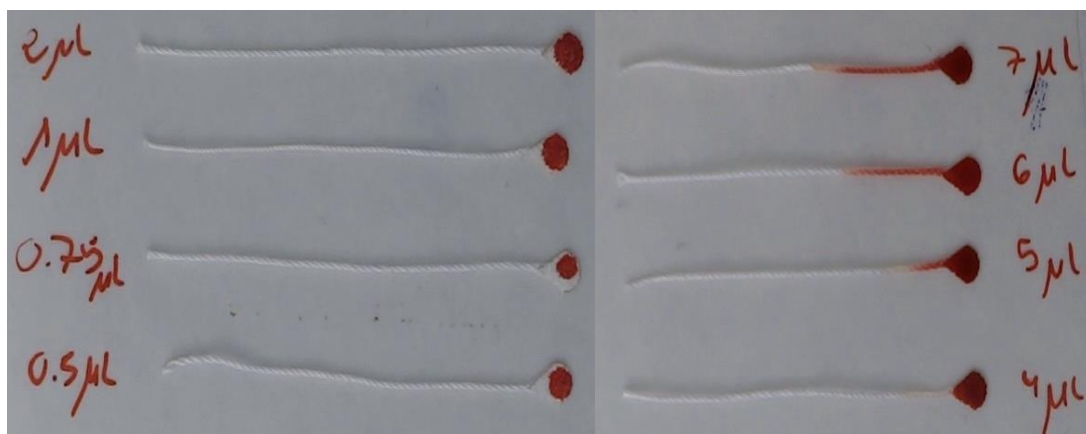


**Figure S10.** RBC separation using a 4 mm tear-shape membrane at different volumes of sample: 7, 6, 5, 4, 3, 2, 1, 0.75 and 0.5  $\mu\text{L}$ .

### 3.10. Whole blood calibration

For calibration the  $\mu\text{TPAD}$  was prepared by adding 2.5  $\mu\text{L}$  of 1xPBS followed by 10 minutes of drying time. Then, 0.5  $\mu\text{L}$  of HRP and GOx solution, 0.5  $\mu\text{L}$  of TMB, and 0.7  $\mu\text{L}$  of chitosan were added and the thread and separating membrane were located in the custom holder. Whole blood spiked samples used for this purpose contained 16, 25, 50, 70, 80, 90, 100, 110, 120 and 130 mg/dL of glucose using 5 replicates per sample by adding 3  $\mu\text{L}$  of whole blood to the device and recording the color change of the device using a smartphone running the app developed. In case of 50, 90 and 110 mg/dL, 10 replicates were performed in order to obtain the precision of the device at different glucose concentrations.

### 3.11. Interfering species

The different interfering species typically found in blood that could influence the recognition or transduction reactions were studied. These were fructose and mannose in the recognition reaction and ascorbic and uric acid in the transduction reaction. To do this,  $\mu\text{TPADs}$  were prepared as described in Section 3.10 on Whole blood calibration, testing whole blood spiked samples containing the interfering species or a mixture of glucose and uric and ascorbic acid. Uric and aspartic acid were also studied

together with glucose, due to its reducing properties, and it was possible to reduce the oxidized colored TMB to its colorless state.

For monosaccharides, the concentration tested was 90 mg/dL, while for uric and ascorbic acid, different quantities were tested in the range of their contents in blood (aspartic acid 1.6, 4.4 and 8.8 mg/dL and uric acid 3.0 and 7.0 mg/dL).

As can be observed in Figures S11 and S12, the interfering species considered do not generate or modify the  $\mu$ TAD signal obtained.

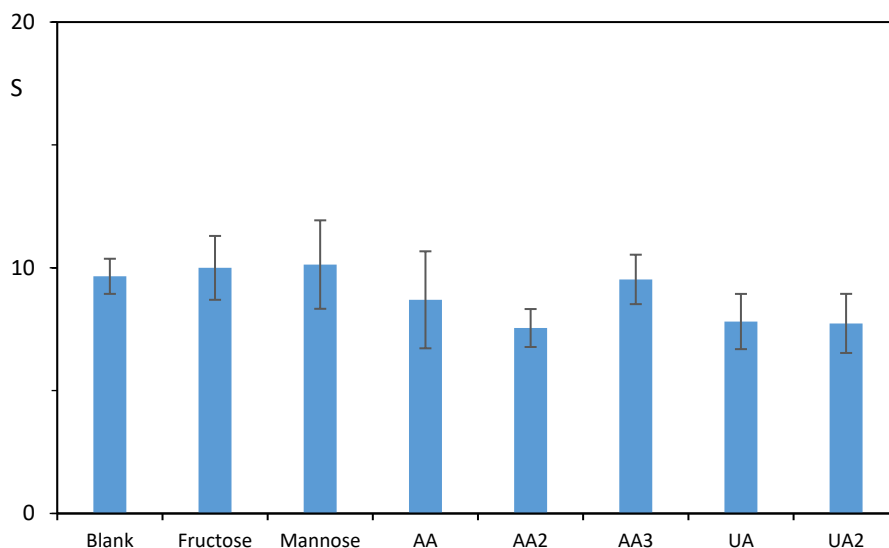


**Figure S.11** Signal obtained when whole blood without glucose is spiked with fructose (90 mg/dL), mannose (90 mg/dL), AA (aspartic acid 1.6 mg/dL), AA2 (aspartic acid 4.4 mg/dL), AA3 (aspartic acid 8.8 mg/dL), UA (30 mg/dL) and UA2 (7.0 mg/dL).

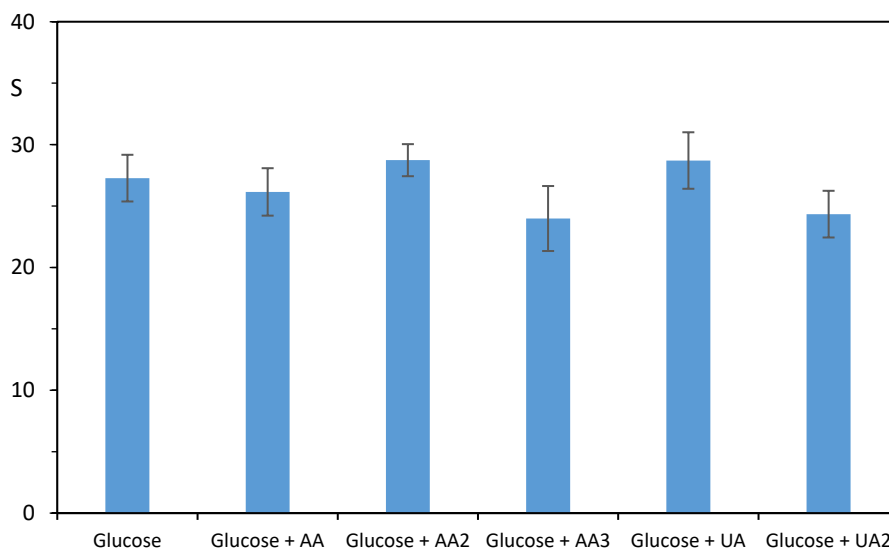


**Figure S.12** Signal obtained when whole blood containing 90 mg/dL in glucose is spiked with fructose (90 mg/dL), mannose (90 mg/dL), AA (aspartic acid 1.6 mg/dL), AA2 (aspartic acid 4.4 mg/dL), AA3 (aspartic acid 8.8 mg/dL), UA (30 mg/dL) and UA2 (7.0 mg/dL).

#### 4. Real samples

For real sample validation, the  $\mu$ TPAD was prepared adding 2.5  $\mu$ L of 1xPBS followed by 10 minutes of drying time. Then, 0.5  $\mu$ L of HRP and GOx solution, 0.5  $\mu$ L of TMB and 0.7  $\mu$ L of chitosan were added, and the thread and separating membrane were located in the custom holder. Then 3  $\mu$ L aliquots of whole blood were added, using 5 different  $\mu$ TPAD per sample, while recording the color change using the smartphone app. A commercial glucose meter analysis was performed on the same samples, and the results were compared in terms of error.

#### 5. Sensor cost

An estimation of the cost of the fabrication of a  $\mu$ TPAD was calculated and is detailed in Table S2.

**Table S2.** Estimated cost of a  $\mu$ TPAD based on the price of the material used to its preparation.

Material (cost per unit)	Quantity used	Assay cost
Thread ( $7.7 \times 10^{-4}$ €/cm)	1.5 cm	$1.16 \times 10^{-3}$ €
Chitosan ( $1.8 \times 10^{-3}$ €/mg)	$1.00 \times 10^{-3}$ mg	$1.76 \times 10^{-6}$ €
HRP ( $4.7 \times 10^{-3}$ €/U)	$1.4 \times 10^{-5}$ U	$6.60 \times 10^{-8}$ €
GOx ( $6.4 \times 10^{-3}$ €/U)	$1.74 \times 10^{-3}$ U	$1.12 \times 10^{-5}$ €
TMB (0.19 €/mg)	$1.75 \times 10^{-3}$ mg	$3.34 \times 10^{-4}$ €
Separation membrane ( $1.4 \times 10^{-4}$ €/mm <sup>2</sup> )	50.00 mm <sup>2</sup>	$7.21 \times 10^{-3}$ €
Metacrilate ( $6.08 \times 10^{-3}$ €/cm <sup>2</sup> )	15.0 cm <sup>2</sup>	$9.12 \times 10^{-2}$ €
Final cost		0.0999 €

**Table S3. Capillary microfluidic devices for glucose analysis.**

Measurement	Support	Detection based chemistry	LOD	Range	Response time	Sample	Reference
Amperometry	Thread	GOx/K <sub>3</sub> [Fe(CN) <sub>6</sub> ]	0.3 mM	1-50 mM	N/A	Water	(Gaines et al., 2018a)
Amperometry	Thread	GOx/K <sub>3</sub> [Fe(CN) <sub>6</sub> ]	2.5 mM	0-15 mM	N/A	Water	(Gaines et al., 2018b)
Amperometry	Thread	GOx/PTB	22.23 μmol/L	75-7500 μmol/L	N/A	Tear	(Agustini et al., 2017)
Colorimetry	Thread	GOx/HRP	0.2 mM	1-7.5 mM	N/A	Artificial urine	(Li et al., 2018)
Colorimetry	Paper	GOx/HRP/Cu <sub>3</sub> (PO <sub>4</sub> ) <sub>2</sub> nanoflowers	25 μM	0.1-10 mM	10 min	Whole blood	(Zhu et al., 2017)
Chemiluminescence	Cloth	Luminol/GOx/HRP	9.07 μM	0.01-10 mM	5 min	Glucose solution	(Li et al., 2017)
Colorimetry	Paper	GOx/HRP	0.5 mM	1-10 mM	15 min	Artificial serum and urine	(Cardoso et al., 2017)
Bipolar electrochemiluminescence	Thread	Luminol/GOx	20.5 μM	0.025-10 mM	N/A	Urine and serum/	(Liu et al., 2017)
Colorimetry	Paper	GOx/HRP/Cu <sub>3</sub> (PO <sub>4</sub> ) <sub>2</sub> nanoflowers	15.6 μM	0 – 300 μM	15 min	Water	(Ariza-Avidad et al., 2016)
Colorimetry	Cloth	GOx/HRP	2.8 mM	3-50 mM	20 min	Artificial urine	(Wu and Zhang, 2015)
<i>Colorimetry</i>	<i>Thread</i>	<i>GOx/HRP</i>	<i>48μM</i>	<i>48-1000 μM</i>	<i>12 s</i>	<i>Water</i>	<i>This work</i>
<i>Colorimetry</i>	<i>Thread</i>	<i>GOx/HRP</i>	<i>28 mg/dL</i>	<i>28 – 130 mg/dL</i>	<i>~10 s</i>	<i>Whole blood</i>	<i>This work</i>

## 6. References

- Agustini, D., Bergamini, M.F., Marcolino-Junior, L.H., 2017. *Biosens. Bioelectron.* 98, 161–167. <https://doi.org/10.1016/j.bios.2017.06.035>
- Ariza-Avidad, M., Salinas-Castillo, A., Capitán-Vallvey, L.F., 2016. *Biosens. Bioelectron.* 77, 51–55. <https://doi.org/10.1016/j.bios.2015.09.012>
- Burtis, A. C., Edwrd, R., Bruns, E. D., 2008. *Fundamentals of Clinical Chemistry :6th Ed, Building.* Elsevier. <https://doi.org/9780721638652>
- Cardoso, T.M.G., de Souza, F.R., Garcia, P.T., Rabelo, D., Henry, C.S., Coltro, W.K.T., 2017. *Anal. Chim. Acta* 974, 63–68. <https://doi.org/10.1016/j.aca.2017.03.043>
- Gaines, M., Gonzalez-Guerrero, M.J., Uchida, K., Gomez, F.A., 2018a. *Electrophoresis* 39, 2131–2135. <https://doi.org/10.1002/elps.201800010>
- Gaines, M., Gonzalez-Guerrero, M.J., Uchida, K., Gomez, F.A., 2018b. *Electrophoresis* 00, 1–5. <https://doi.org/10.1002/elps.201800348>
- Li, H., Wang, D., Liu, C., Liu, R., Zhang, C., 2017. *RSC Adv.* 7, 43245. <https://doi.org/10.1039/c7ra06721f>
- Li, Y.D., Li, W.Y., Chai, H.H., Fang, C., Kang, Y.J., Li, C.M., Yu, L., 2018. *Cellulose* 25, 4831–4840. <https://doi.org/10.1007/s10570-018-1891-3>
- Liu, R., Liu, C., Li, H., Liu, M., Wang, D., Zhang, C., 2017. *Biosens. Bioelectron.* 94, 335–343. <https://doi.org/10.1016/j.bios.2017.03.007>
- Wu, P., Zhang, C., 2015. *Lab Chip* 15, 1598–1608. <https://doi.org/10.1039/C4LC01135J>
- Zhu, X., Huang, J., Liu, J., Zhang, H., Jiang, J., Yu, R., 2017. *Nanoscale* 9, 5658–5663. <https://doi.org/10.1039/C7NR00958E>